THE JOURNAL OF BIOLOGICAL CHEMISTRY VOL. 280, NO. 48, pp. 39786–39794, December 2, 2005

Role of Endogenous TRPC6 Channels in Ca^{2+} Signal Generation in A7r5 Smooth Muscle Cells*

Received for publication, June 3, 2005, and in revised form, September 1, 2005 Published, JBC Papers in Press, October 3, 2005, DOI 10.1074/jbc.M506064200

Jonathan Soboloff[‡1], **Maria Spassova**[‡1], **Wen Xu**[‡], **Li-Ping He**[‡], **Natalia Cuesta**[§], **and Donald L. Gill**[‡2]

From the [‡]*Department of Biochemistry and Molecular Biology and the* [§]*Department of Microbiology and Immunology, University of Maryland School of Medicine, Baltimore, Maryland 21201*

The ubiquitously expressed canonical transient receptor potential (TRPC) ion channels are considered important in Ca^{2+} signal generation, but their mechanisms of activation and roles remain elusive. Whereas most studies have examined overexpressed TRPC channels, we used molecular, biochemical, and electrophysiological approaches to assess the expression and function of endogenous TRPC channels in A7r5 smooth muscle cells. Real time PCR and Western analyses reveal TRPC6 as the only member of the diacylglycerol-responsive TRPC3/6/7 subfamily of channels expressed at significant levels in A7r5 cells. TRPC1, TRPC4, and TRPC5 were also abundant. An outwardly rectifying, nonselective cation current was activated by phospholipase C-coupled vasopressin receptor activation or by the diacylglycerol analogue, oleoyl-2-acetyl-*sn*-glycerol (OAG). Introduction of TRPC6 small interfering RNA sequences into A7r5 cells by electroporation led to 90% reduction of TRPC6 transcript and 80% reduction of TRPC6 protein without any detectable compensatory changes in the expression of other TRPC channels. The OAG-activated nonselective cation current was similarly reduced by TRPC6 RNA interference. Intracellular Ca^{2+} measurements using fura-2 revealed that thapsigargin-induced store-operated Ca^{2+} entry was unaffected by TRPC6 knockdown, whereas vasopressin-induced Ca^{2+} entry was suppressed by more than 50%. In contrast, OAG-induced Ca^{2+} transients were unaffected by TRPC6 knockdown. Nevertheless, OAG-induced Ca^{2+} entry bore the hallmarks of TRPC6 function; it was inhibited by protein kinase C and blocked by the Src-kinase inhibitor, 4-amino-5-(4-chlorophenyl)-7-(*t*-butyl)pyrazolo[3,4-d]pyrimidine (PP2). Importantly, OAG-induced Ca^{2+} entry was blocked by the potent L-type Ca^{2+} channel inhibitor, nimodipine. Thus, TRPC6 activation probably results primarily in Na^+ ion entry and depolarization, leading to activation of L-type channels as the mediators of Ca^{2+} entry. Calculations reveal that even 90% reduction of TRPC6 channels would allow depolarization sufficient to activate L-type channels. This tight coupling between TRPC6 and L-type channels is probably important in mediating smooth muscle cell membrane potential and muscle contraction.

Receptor-induced Ca^{2+} signals are crucial to the function of all cells (1) and involve both release of Ca^{2+} from stores and entry of Ca^{2+} through plasma membrane channels (1–3). Although identification of the latter has proven elusive, members of the canonical transient receptor potential (TRPC)[3] channel family have been leading contenders (2–5). The TRPC channels all appear to be activated in response to phospholipase C (PLC)-coupled receptors (2–8). Within the TRPC family, there are two structurally divided subgroups: TRPC3, TRPC6, and TRPC7 channels (TRPC3/6/7) and TRPC1, TRPC4, and TRPC5 (TRPC1/4/5). One functional characteristic distinguishing these two subgroups is the ability of diacylglycerol (DAG) to activate TRPC3/6/7 channels but not TRPC1/4/5 channels (2, 6–11). DAG also activates TRPC2 channels; however, this channel is not expressed in higher mammals and is restricted mostly to the vomeronasal organ (12). As a product of receptor-induced PLC activation, DAG is an obvious mediator of TRPC channel activation. However, its role in the activation of endogenously expressed TRPC3/6/7 channels is uncertain (7, 8, 13–15). The majority of studies revealing the action of DAG on TRPC channels have been undertaken using overexpression systems (2, 7, 8, 14, 15). Such expression may differ from endogenous TRPC expression. For example, considering that TRPC channels probably function as tetramers (4, 5), overexpression may result in a predominance of homotetrameric structures, whereas endogenous expression may reflect heteromers between TRPC channel subtypes, resulting in quite different properties (2, 4, 5). In addition, since TRPC channels may function within organized signaling domains (2, 16), endogenously expressed TRPC channels may be assembled along with adaptor and/or regulatory proteins, the association of which may be quite different when overexpressed (2, 11, 16–18). Hence, there is a need to examine the activation and function of endogenously expressed TRPC channels.

Whereas TRPC channels are ubiquitously expressed among cell types, there are surprisingly few reports describing the functional role of native TRPC channels. For example, TRPC3 channels are highly expressed in pontine neurons and mediate a nonselective cation current in response to the neurotrophin receptor, TrkB (19). TRPC2 channels appear to mediate the primary electrical response to pheromones in the vomeronasal organ of most mammals except higher primates (12). The TRPC6 channel is highly expressed in a number of different smooth muscle cell types (20–22), and there have been studies indicating that it plays a role in receptor-induced Ca^{2+} signaling in smooth muscle (20–23). In primary portal vein myocytes, current closely corresponding to overexpressed TRPC6 channels was reduced by treatment with TRPC6 antisense oligonucleotides (20). Down-regulation of TRPC6 by antisense sequences in pulmonary vascular smooth muscle cells resulted in reduction of store-operated Ca^{2+} entry (21). Using the clonal A7r5 aortic-derived smooth muscle cell line, Jung *et al.* (22) described a TRPC6-

* This work was supported by National Institutes of Health Grants HL55426 and AI058173 and the Interdisciplinary Training Program in Muscle Biology, University of Maryland School of Medicine. The costs of publication of this article were defrayed in part by the payment of page charges. This article must therefore be hereby marked "*advertisement*" in accordance with 18 U.S.C. Section 1734 solely to indicate this fact.

[1] These authors contributed equally to this work.

[2] To whom correspondence should be addressed: Dept. of Biochemistry and Molecular Biology, University of Maryland School of Medicine, 108 North Greene St., Baltimore, MD 21201. Tel.: 410-706-2593 (office) or 410-706-7247 (laboratory); Fax: 410-706-6676; E-mail: dgill@umaryland.edu.

[3] The abbreviations used are: TRPC, canonical transient receptor potential; VP, vasopressin; PLC, phospholipase C; PKC, protein kinase C; $InsP_3$, inositol 1,4,5-trisphosphate; DAG, diacylglycerol; OAG, oleoyl-2-acetyl-*sn*-glycerol; PMA, phorbol 12-myristate 13-acetate; SERCA, sarcoplasmic/endoplasmic reticulum Ca^{2+} ATPase; PP2, 4-amino-5-(4-chlorophenyl)-7-(*t*-butyl)pyrazolo[3,4-d]pyrimidine; siRNA, short interfering RNA sequence; RNAi, RNA interference.

like current activated by the permeant diacylglycerol analogue, oleoyl-2-acetyl-*sn*-glycerol (OAG). In this case, the current was enhanced by PLC-coupled receptor activation but was not modified by Ca^{2+} store depletion (22). In recent studies using TRPC6 knockout mice, a phenotype of *increased* arterial blood pressure, augmented arterial tone, and enhanced agonist- and DAG-induced current in smooth muscle was observed (6–8, 24). Whereas such knockout would be expected to prevent rather than augment the Ca^{2+}-mediated responses, there appeared to be an overcompensatory increase in expression of the closely related TRPC3 channel (6–8, 24).

The primary role of Ca^{2+} entry in controlling smooth muscle contraction and the possible role of TRPC channels in these responses prompted us to examine the presence and possible function of TRPC channels using A7r5 cells. A careful examination of the expression of TRPC channels at both transcript and protein levels reveals that, of the closely rated TRPC3/6/7 subfamily members, only TRPC6 channels are detected. This provides a system in which the function of endogenously expressed TRPC6 channels can be examined in relative isolation from the other subfamily members, TRPC3 and TRPC7. Using an RNAi knockdown approach, we have identified TRPC6 channel function in A7r5 cells and reveal that the channel may be more important as a mediator of Na^+ ion entry resulting in the activation of voltage-dependent Ca^{2+} entry channels.

EXPERIMENTAL PROCEDURES

Cells and RNAi—Rat aortic smooth muscle A7r5 cells, passage 10–25, were cultured in Dulbecco's modified Eagle's medium supplemented with fetal bovine serum (10%), penicillin, and streptomycin as described previously (17, 25). For TRPC6 knockdown studies, A7r5 cells were mixed with 200 nM TRPC6 siRNA (GCAGCAUCAUUCAUUGCAAGAUUUA or GGAAUAUGCUUGACUUUGGAAUGUU) or a control sequence (GCAACUAACUUCGUUAGAAUCGUUA), each with its complementary sequence. We used Stealth (Invitrogen) siRNA sequences developed to eliminate nonspecific stress responses of the PKR/interferon pathway induced by siRNA. Cells together with siRNA sequences were electroporated using the Gene Pulser II electroporation system (Bio-Rad) at 350 V, 960 microfarads, and infinite resistance. After a 3-h recovery period in serum-free Opti-MEM, 10% fetal bovine serum was added, and cells were incubated for 40 h on coverslips before fura-2 imaging of electrophysiology measurements was undertaken.

Real Time PCR—Real time quantitative PCR was performed in a Sequence Detector System (ABI Prism 7900 Sequence Detection System and software; PerkinElmer Life Sciences). Amplification was performed in a final volume of 25 μl, containing 30 ng of cDNA from the reverse transcribed reaction, primer mixture (0.3 μM each of sense and antisense primers), and 12.5 μl 2× SYBR Green Master Mix (Applied Biosystems). The oligonucleotide primers shown in TABLE ONE were designed using Primer Express 2.0 software (Applied Biosystems). The standard amplification program included 40 cycles of two steps, each comprising heating to 95 °C and heating to 60 °C. Fluorescent product was detected at the last step of each cycle. In order to verify the purity of the products, a melting curve was produced after each run. To determine the relative quantitation of gene expression, the comparative threshold cycle method (ΔC_T) was used (26). To control for variation in RNA quantity and quality, we used 18 S ribosome RNA as an internal control to calculate a relative C_t for the target molecules (TRPC channels) of interest. Subtracting the C_T of the housekeeping gene from the C_T of the gene of interest yields the ΔC_T. A serially diluted positive control sample (rat brain) was analyzed by linear regression to determine the sensitivity and linearity of the assay. The final mRNA levels were normalized according to their C_t values from the standard curves.

Western Blot Procedures—To detect TRPC expression, A7r5 cells were lysed in chilled Nonidet P-40 buffer (1% (v/v) Nonidet P-40, 150 mM NaCl, 50 mM Tris-HCl, pH 8.0, containing 100 μM phenylmethylsulfonyl fluoride and Sigma protease inhibitor mixture I) followed by an incubation period of 30 min at 4 °C. Following centrifugation (18,000 × *g*, 20 min at 4 °C), the protein content of the supernatants was quantified using Bio-Rad DC protein assay kits. For rat brain, tissue was homogenized in Nonidet P-40 buffer in exactly the same manner as above for A7r5 cells. For both A7r5 and rat brain, protein extracts (15 μg/lane of each) were resolved on 6% SDS-polyacrylamide gels (27) and electroblotted onto Bio-Rad nitrocellulose membranes (Bio-Rad) (28). After transfer, the nitrocellulose membranes were blocked (l h, room temperature) in Tris-buffered saline-Tween 20 (TBST; 10 mM Tris-HCl, pH 8.0, 150 mM NaCl, 0.1% Tween 20) containing membrane blocking agent (5%) (Amersham Biosciences) and subsequently incubated overnight at 4 °C with rabbit anti-TRPC1, -TRPC4, -TRPC5, or -TRPC6 antibodies, with rabbit anti-TRPC3 antibody, or with goat anti-TRPC7. Membranes were then washed two times (7 min) in TBST and incubated with secondary antibody (30 min; goat anti-rabbit or donkey anti-goat IgG conjugated to horseradish peroxidase diluted 1:2500 in TBST). Subsequently, membranes were washed three times (5 min) in TBST followed by a single wash (5 min) in Tris-buffered saline (TBS; 150 mM NaCl, 10 mM Tris-HCl, pH 8.0). Peroxidase activity was visualized using the ECL kit as according to the manufacturer's instructions (Amersham Biosciences).

Intracellular Ca^{2+} Measurements—Cells grown on coverslips were placed in external solution (107 mM NaCl, 7.2 mM KCl, 1.2 mM $MgCl_2$, 11.5 mM glucose, 20 mM Hepes-NaOH, pH 7.2; this solution is "cation-safe," free of sulfate and phosphate anions) and loaded with fura-2/acetoxymethylester (2 μM) for 30 min at 20 °C. Cells were washed, and dye was allowed to de-esterify for a minimum of 30 min at 20 °C. Approximately 95% of the dye was confined to the cytoplasm as determined by the signal remaining after saponin permeabilization (29). Cells on coverslips were placed in external solution in the absence or presence of 3 mM $CaCl_2$, as described earlier (10, 30). Ca^{2+} measurements were made using an InCyt dual wavelength fluorescence imaging system (Intracellular Imaging Inc.). Fluorescence emission at 505 nm was monitored with excitation at 340 and 380 nm; intracellular Ca^{2+} measurements are shown as 340/380 nm ratios obtained from groups (6–12) of single cells. The details of these Ca^{2+} measurements were described previously (31). Resting Ca^{2+} levels in A7r5 cells were 100–200 nM (32). All measurements shown are representative of a minimum of three and in most cases a larger number of independent experiments.

Whole Cell Patch Clamp Measurements—For patch clamp experiments, A7r5 cells grown on glass coverslips were transferred to the recording chamber and kept in a standard external solution (145 mM NaCl, 2.8 mM KCl, 10 mM CsCl, 2 mM $MgCl_2$, 10 mM glucose, 0.2 mM EGTA, 10 mM HEPES-NaOH, pH 7.40. Free Ca^{2+} was adjusted to 50 μM using WEBMAXC software). Patch clamp experiments were conducted in the tight seal whole cell configuration. High resolution current recordings were acquired with a computer-based patch clamp amplifier system (EPC-10, HEKA, Lambrecht, Germany). Patch pipettes had resistances between 2 and 4 MΩ after filling with the standard pipette solution (145 mM cesium glutamate, 8 mM NaCl, 2 mM ATP, 0.3 mM GTP, 10 mM EGTA, adjusted with CsOH to pH 7.2). Free Mg^{2+} was adjusted to 1 mM, and free Ca^{2+} was adjusted to 100 nM with $MgCl_2$ and $CaCl_2$ using WEBMAXC software. Immediately after establishment of the whole cell configuration, voltage ramps of 50-ms duration spanning

TABLE ONE

Oligonucleotide sequences of primers used for real time reverse transcription-PCR

Target	GenBank™ accession number	Orientation	Sequence (5′–3′)	Predicted size	Nucleotide location
				bp	
TRPC1	AF061266	Forward	CGACACCTTCCACTCGTTCA	64	1716–1780
		Reverse	GCGCTAAGGAGAAGATGTACCAGA		
TRPC2	NM017011	Forward	GTTCCAGTTTCTCTTCTGGACCAT	190	1804–1994
		Reverse	CAGCATCGTCCTCGATCTTCT		
TRPC3	AB022331	Forward	CATGCAGTGCAAAGACTTCGTAG	74	531–605
		Reverse	TTCAGAATGGCTTCCACCTCTT		
TRPC4	NM_080396	Forward	CTCTGCAGATATCTCTGGGAAGAAT	67	1514–1581
		Reverse	CACGAGGCAGTATATGAATAAGAACTTT		
TRPC5	AY064411	Forward	TGAAACCCTTCAGTCACTCTTCTG	102	2038–2140
		Reverse	AGTAGCTCCCACAAACTCCGTG		
TRPC6	NM_053559	Forward	AGTGTACAGAATGCAGCCAGAAAC	79	758–837
		Reverse	CAGCCCTTTGTAGGCATTGATC		
TRPC7	XM_225159	Forward	CCCTTTAACCTGGTGCCGA	113	2665–2778
		Reverse	TGGAGTTCAGCATGCCCATT		

the voltage range of −100 to +100 mV were delivered from a holding potential of 0 mV at a rate of 0.5 Hz. All voltages were corrected for a liquid junction potential of 10 mV between external and internal solutions. Currents were filtered at 2.3 kHz and sampled at 20-μs intervals. Capacitive currents and series resistance were determined and corrected using the automatic capacitance and series resistance compensation of the EPC-10. For analysis, four ramps were averaged after current inactivation and used for leak subtraction. The low resolution temporal development of inward currents (at −80 mV) and outward current (80 mV) was leak-corrected with an individual ramp current record after current inactivation by measuring the current amplitude at −80 and 80 mV. Estimates of leak development in untreated cells measured over 300 s revealed a linear decrease in leak current of no more than 1 pA per 30 s. OAG and VP were added to the standard external solution as indicated.

Materials and Miscellaneous Procedures—Thapsigargin, PP2, GF-109203X, and OAG were from EMD Biosciences (San Diego, CA). Fura-2/acetoxymethylester was from Molecular Probes, Inc. (Eugene, OR). Vasopressin was from Sigma. Rabbit anti-TRPC1, -TRPC4, -TRPC5, or -TRPC6 antibodies were from Alomone Labs (Israel), and rabbit anti-TRPC3 was a generous gift from Dr. Randen Patterson (Penn State University). Goat anti-TRPC7 was from Santa Cruz. Goat anti-rabbit and donkey anti-goat IgG conjugated to horseradish peroxidase were from Jackson Laboratories. The A7r5 cell line was from ATCC (Manassas, VA).

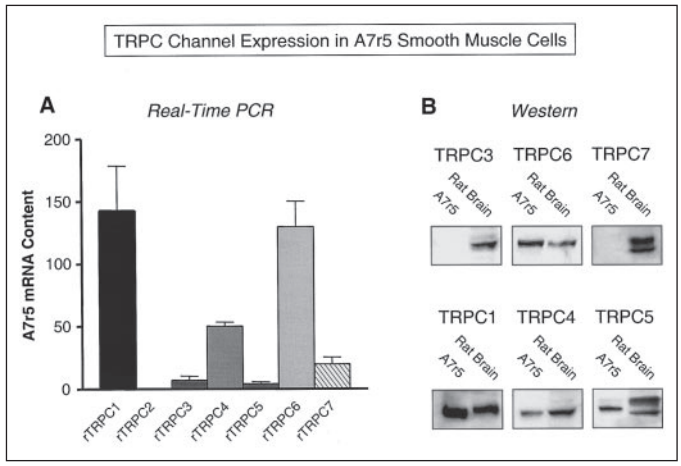

FIGURE 1. **TRPC channel expression in rat aortic A7r5 smooth muscle cells.** A7r5 cells maintained under optimal growth conditions were collected, lysed, and analyzed for TRPC expression. *A*, primers for real time PCR were designed against unique regions of each member of the TRPC family (TABLE ONE) and compared against an internal control (18 S ribosomal RNA). Total mRNA content is expressed as arbitrary units. *B*, expression of the TRPC3/6/7 and TRPC/1/4/5 subfamilies of channels were assessed by Western blot. Rat brain extracts were used as a standard to determine antibody specificity and relative TRPC content.

RESULTS AND DISCUSSION

TRPC Channel Profile—TRPC channels have been postulated to serve widely among cells types as mediators of Ca^{2+} entry in response to PLC-coupled receptors (2, 4). Receptor-mediated Ca^{2+} entry signals play a prominent role in smooth muscle, and we sought to assess the role of TRPC channels using the well studied A7r5 smooth muscle cell line (17, 32). Our focus has been on the widely expressed TRPC3/6/7 group of channels known to be activated by the PLC product, DAG (2, 9, 29, 30, 33). Crucial to assessment of the function to these channels was an accurate quantitative analysis of the expression pattern for TRPC channels in A7r5 cells. TRPC channel message has previously been reported in A7r5 cells by Northern hybridization analysis (22); however, TRPC protein expression has not been examined. We designed primers for each TRPC family member (TABLE ONE) and quantitatively analyzed levels of expression of TRPC message using real time PCR (Fig. 1*A*). Our analyses reveal that TRPC1 and TRPC6 are the predominant TRPC channel mRNAs observed in A7r5 cells. However, in contrast to the earlier Northern analysis (22), we detected significant levels of TRPC4 and TRPC7 message. TRPC3 and TRPC5 mRNA levels were barely detectable, whereas no TRPC2 mRNA was detected. The latter is unsurprising since TRPC2 is only reported expressed in vomeronasal organ (14), erythroid precursor cells (34), and sperm (35). Western analysis of TRPC protein levels in A7r5 cells is shown in Fig. 1*B*. The reliability of TRPC antibodies has been inconsistent among TRPC subtypes, and we confirmed their effectiveness by their identification of TRPC channels in rat brain extracts in which high levels of most TRPC channels are present (Fig. 1*B*). In A7r5 cells, TRPC1 and TRPC6 were expressed at levels equivalent to those observed in rat brain, consistent with the real time PCR analysis. Certainly, both proteins were prominent in A7r5 cells. TRPC4 and TRPC5 protein levels were also quite prominent, a result not predicted from their relative mRNA levels. Whereas the size

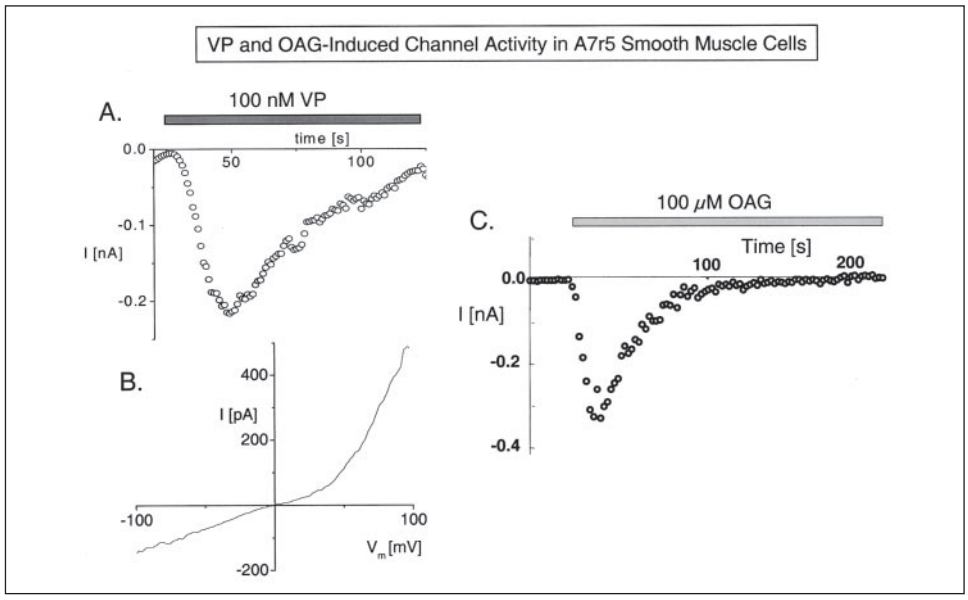

FIGURE 2. **Vasopressin- and OAG-induced nonselective currents in A7r5 cells.** Nonselective cation currents in A7r5 cells were measured in the presence of 1 μM nimodipine in the whole cell configuration. *A*, the time course of vasopressin-induced inward current recorded at −80 mV in A7r5 cells. *B*, the current-voltage relationship of vasopressin-induced current measured at the time of maximal activation as determined in *A*. The outward current carried by Cs^+ ions and the reversal potential of 0 mV indicate the nonselective properties of the channels. *C*, the time course of OAG-induced inward current measured at −80 mV.

of TRPC5 appeared distinct from the doublet recognized in brain, a large decrease in the intensity of this band occurred after TRPC5 RNAi, confirming its authenticity (not shown). Significantly, no TRPC3 or TRPC7 protein could be detected despite the presence of prominent bands for each channel in rat brain, indicating the effectiveness of the antibodies used. This does not mean that the TRPC3 and TRPC7 proteins are absent, but their expression level is beneath our minimum detection limit. Although the relative levels of different TRPC channels are difficult to ascertain from Western analyses, it is clear that significant disparities exist between levels of protein and mRNA expression. Such differences are probably explained by the relative stability and turnover of both message and protein. Despite the quantitative uncertainty of Western analysis, assessment of TRPC protein levels rather than mRNA levels is obviously a more reliable indicator of the presence and relative levels of endogenous TRPC channels. In a paper published after completion of this work, Moneer *et al.* (36) revealed significant variations in the expression of TRPC channels in different strains of A7r5 cells. In certain strains, significant levels of TRPC3 message could be detected, although no information on protein levels was given. Considering that A7r5 cells are derived from rat aortic smooth muscle, which does not express TRPC3 (8), it is possible that certain strains have undergone alteration during lengthy passaging.

Vasopressin and OAG-induced Currents in A7r5 Cells—From these data, TRPC6 is the only detectable member of the TRPC3/6/7 subgroup of TRPC channels expressed in A7r5 cells. Hence, A7r5 cells offer a useful system to study the DAG responsiveness of endogenous TRPC6 channels. Recent studies have revealed that the permeant DAG analogue, OAG, can stimulate an inward current in smooth muscle cells (20, 23). Whereas it is established that exogenously expressed TRPC6 channels are responsive to OAG (9, 10), it remains unclear whether endogenously expressed TRPC6 channels respond similarly (13, 14). We compared PLC-coupled VP receptor-mediated and OAG-induced channel activities in A7r5 cells using the whole cell patch clamp configuration, replacing K^+ with Cs^+ to block K^+ channels and using nimodipine (1 μM) to block L-type Ca^{2+} channels (Fig. 2). Application of 1 μM VP to the bath induced a nonselective cation current in A7r5 cells. The time course for VP-induced current at −80 mV (Fig. 2*A*) revealed inward current detectable within a few seconds of VP addition and rising to a maximum within ~30 s and declining thereafter. The current/voltage dependence (Fig. 2*B*) of this VP-induced current revealed a pattern of outward rectification and a reversal potential of 0 mV. A similar inward current was activated in response to application of 100 μM OAG (Fig. 2*C*). However, the *I*/V relationship for OAG-induced current (see Fig. 4) was subtly different, exhibiting double rectifying properties similar to the properties of TRPC6 channels expressed in a number of different systems (5). We sought to undertake a more rigorous determination of the identity of the channel activity mediating this current by gene silencing approaches.

Knockdown of TRPC6 Using siRNA—In order to determine the role of TRPC6 in OAG- and VP-induced channel activity, an electroporation protocol was utilized to introduce selected stealth siRNA sequences (see "Experimental Procedures"). As shown in Fig. 3, introduction of double-stranded RNA sequences corresponding to nucleotides starting at 1574 or 1609 resulted in substantial reduction in TRPC6 expression. Real time PCR revealed an approximate 90% reduction of TRPC6 mRNA levels within 15 h as compared with a control sequence (Fig. 3*A*). Based on a time course of protein expression by Western analysis, we determined that maximal down-regulation of the protein was at 72 h after electroporation of 200 nM siRNA. At this time, densitometric analysis of Western blots revealed a 70–90% decrease in TRPC6 protein expression (Fig. 3*B*). Important was to examine the changes in the expression levels of other TRPC family members. Compensation by related subfamily members can severely complicate analysis of a phenotype, using either gene knockout in whole animals (6) or gene silencing techniques (37). In particular, in recent studies with TRPC6 knockout mice, there appears to be a compensatory expression of TRPC3 channels, which may account for increased smooth muscle cell tone in the knockout animals (6–8, 24). Thus, examination of the expression levels of other TRPC3/6/7 channel members was of particular interest. As shown in Fig. 3*A*, the levels of message for TRPC1, TRPC3, TRPC5, and TRPC7 were virtually unaffected in the same cells in which TRPC6 knockdown was highly effective. At the protein level, there were no detectable changes in the expression of these same TRPC channel members (Fig. 3*C*). It is important to qualify this interpretation for TRPC3 and TRPC7, which are expressed at low levels. Whereas we can make no assertion about any changes in expression of TRPC3 and TRPC7 based on protein determinations that were below detection limits, the message for these channels *was* detectable and revealed no change. Thus, the ability to

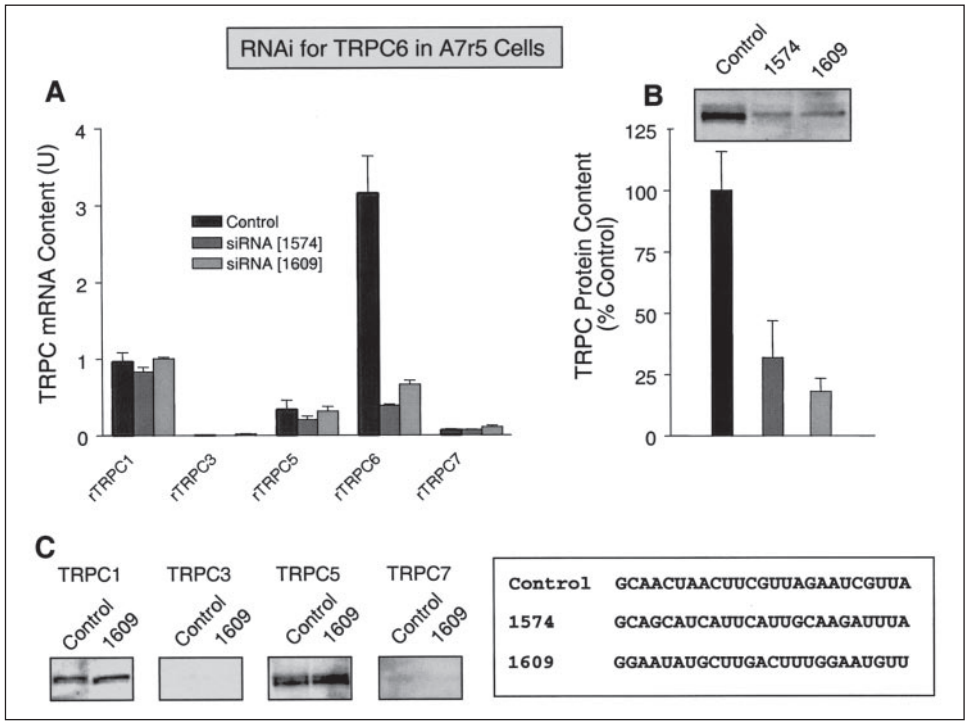

FIGURE 3. **TRPC expression patterns in A7r5 cells treated with TRPC6 siRNA.** Knockdown of TRPC6 was achieved by electroporation to transfect siRNA or control sequences (see *box*) into A7r5 cells. *A*, primers for real time PCR were designed against unique regions of each member of the TRPC family and compared against an internal control (18 S ribosomal RNA). Total mRNA content is expressed as arbitrary units. A significant decrease in TRPC6 mRNA content was revealed 15 h after electroporation. No significant changes in the expression of other TRPC channels were detected. *B*, a maximal decrease of TRPC6 protein expression was detected 40–64 h after electroporation by Western blot analysis. *C*, the expression of TRPC1, TRPC3, TRPC5, and TRPC7 channels were unaltered by TRPC6 knockdown. The "1609" siRNA sequence was used for this and subsequent experiments.

decrease TRPC6 expression in this system without significant compensatory changes in other TRPC channels provides an important advantage in analyzing the role of endogenous TRPC6 channels.

Effect of TRPC6 Knockdown on OAG-induced Current—Whole cell recordings of A7r5 cells revealed a substantial decrease in the OAG-induced current after treatment with siRNA for TRPC6. As shown in Fig. 4*A*, the development of peak inward current (measured at −80 mV) was substantially reduced in cells treated with the 1609 siRNA as compared with cells treated with control siRNA. The current-voltage relationship shown in Fig. 4*B* reveals that both inward and outward current are reduced. The outward current (measured at 80 mV) was reduced on average by more than 80% (Fig. 4*C*), which is consistent with the reduction in protein observed with siRNA (Fig. 3). Whereas the OAG-induced peak was greatly diminished, a small residual current developed more slowly. Since the other OAG-inducible TRPC channels, TRPC3 and TRPC7, were not detectable even after TRPC6 knockdown (Fig. 3), it is unlikely that this current is related to increased expression of other TRPC channels. Instead, this slower activating residual current might reflect a distinct TRPC6 heteromer resulting from the decreased proportion of TRPC6 *versus* other TRPC channels. Alternatively, it may reflect other channels perhaps sensitive to OAG through a PKC-dependent process.

Effects of TRPC6 Knockdown on Store-operated and Receptor-induced Ca^{2+} Entry—Since TRPC channels have been widely implicated in mediating store-operated and receptor-dependent Ca^{2+} entry (1–5), the role of TRPC6 in mediating Ca^{2+} entry in A7r5 cells was important to ascertain. We initially examined the effects of RNAi for TRPC6 on store-operated Ca^{2+} entry induced by emptying stores with the SERCA pump blocker, thapsigargin. Blockade of the SERCA pump results in passive release of Ca^{2+} from stores, and upon the addition of Ca^{2+} to the outside medium, a substantial entry of Ca^{2+} is observed. As shown in Fig. 5, *A–C*, there was no significant effect of TRPC6 knockdown on either the amount of Ca^{2+} released by thapsigargin or on the store-operated channel-mediated Ca^{2+} entry ($p > 0.05$). This is a significant result, indicating that the TRPC6 channel is playing little role in purely

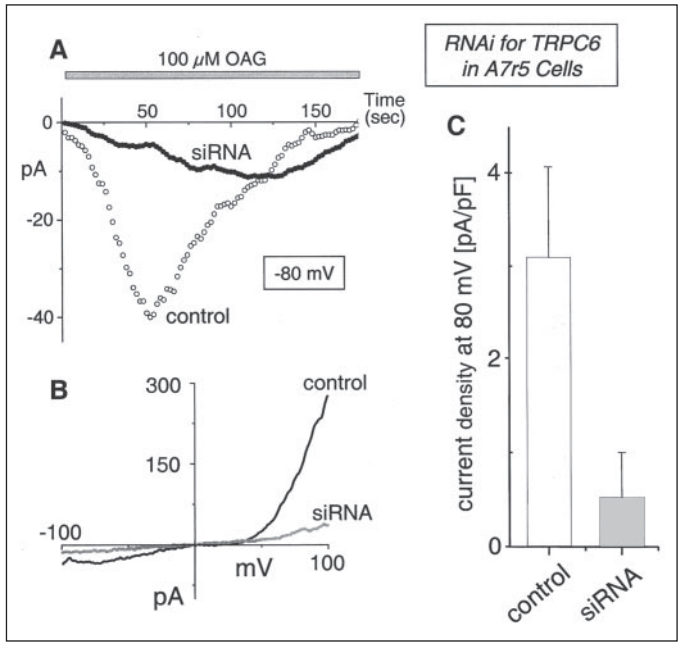

FIGURE 4. **Inhibition of OAG activated current in A7r5 cells by TRPC6 siRNA.** Nonselective cation currents in A7r5 cells were measured in the presence of 1 μM nimodipine in the whole cell configuration 40–64 h after transfection by electroporation of TRPC6 "1609" siRNA or a scrambled siRNA control. *A*, the addition of OAG to A7r5 cells at a holding potential of −80 mV led to current activation that was almost abolished in TRPC6 siRNA-treated cells. *B*, the current-voltage relationship of OAG-induced current measured at the time of maximal activation determined in *A*. The I/V curve shows a double-rectifying property typical for TRPC6. siRNA inhibition reveals a large reduction in the outward as well as the inward current. *C*, analysis of the outward current, which was greater in magnitude, revealed an ~90% decrease in TRPC6 knockdown cells.

store-operated Ca^{2+} entry. We have stressed recently that the complete emptying of stores effected by thapsigargin, while important for observing purely store-operated Ca^{2+} entry, is not a condition encountered physiologically (2, 11, 14, 17, 18, 38). Thus, we also examined the effects of TRPC6 knockdown on Ca^{2+} signals induced by activation of the

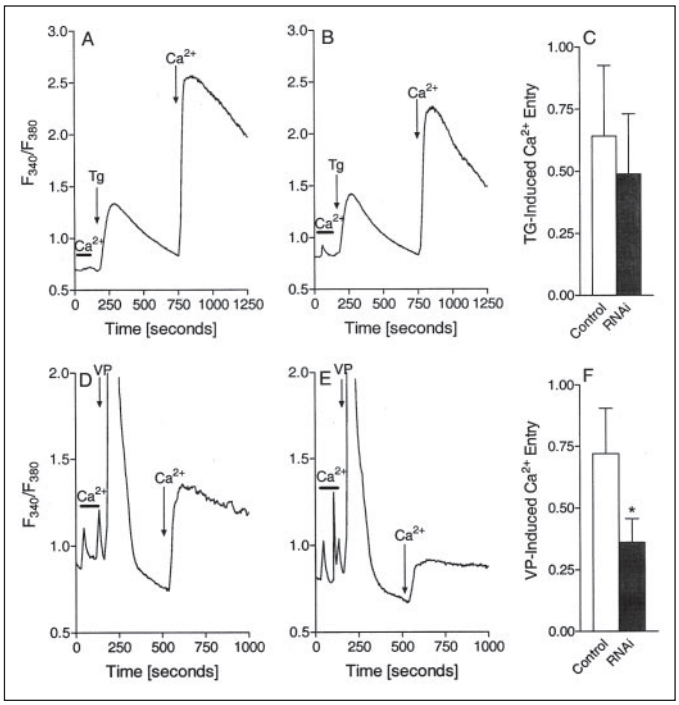

FIGURE 5. **Effects of TRPC6 knockdown on store-operated and vasopressin-induced Ca^{2+} entry.** Fura-2-loaded A7r5 cells were examined 40–64 h after electroporation with either a scrambled control sequence or TRPC6 "1609" siRNA, at which time maximal knockdown of TRPC6 protein was observed. 2 μM thapsigargin (*TG*; *A–C*) or 100 nM vasopressin (*VP*; *D–F*) was added in the absence of extracellular Ca^{2+} (*arrow*). Ca^{2+} entry was assessed by the addition of 3 mM Ca^{2+}, both before and after exposure to VP or thapsigargin. *C*, no significant differences ($p > 0.05$) were detected in the amount of thapsigargin-induced Ca^{2+} entry in control and TRPC6 siRNA-treated cells ($n = 5$). *F*, VP-induced Ca^{2+} entry was reduced by 50% ($p < 0.02$) in TRPC6 siRNA-treated cells as compared with control cells ($n = 6$).

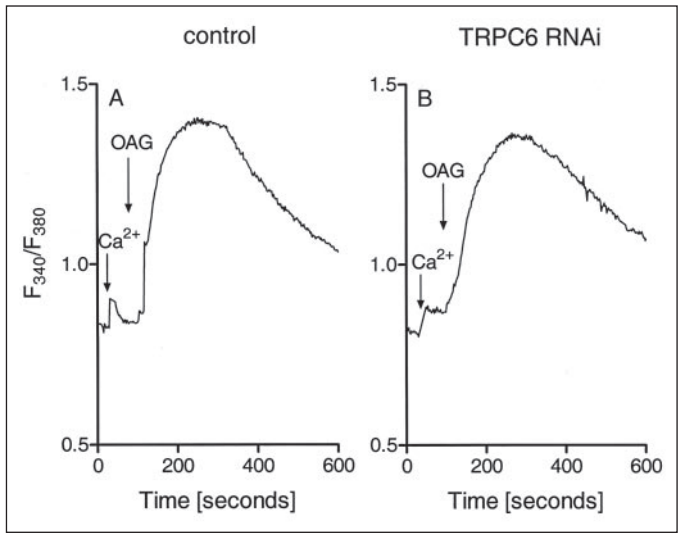

FIGURE 6. **Knockdown of TRPC6 failed to suppress OAG-induced Ca^{2+} entry.** Fura-2-loaded A7r5 cells were examined 40–64 h after electroporation (at which time maximal knockdown of TRPC6 protein was observed) with a scrambled control sequence (*A*) or TRPC6 "1609" siRNA (*B*). 100 μM OAG was added in the presence of 3 mM Ca^{2+}. TRPC6 knockdown had no apparent effect on OAG-induced Ca^{2+} entry.

physiologically more relevant PLC-coupled vasopressin receptor. As shown in Fig. 5*D*, vasopressin induced a rapid $InsP_3$-mediated Ca^{2+} release from intracellular stores in the absence of extracellular Ca^{2+}. Upon the addition of Ca^{2+} to the external medium, Ca^{2+} entry is observed, representing a combination of receptor-induced and store-operated Ca^{2+} entry (2, 11, 17). When undertaken on TRPC6 siRNA-treated cells (Fig. 5*E*), Ca^{2+} release was unaffected, but Ca^{2+} entry was significantly reduced ($p < 0.02$) by an average of 50%, based upon six separate experiments, each including 6–12 cells (Fig. 5*F*). It should be noted that in A7r5 cells, the addition of external Ca^{2+} prior to vasopressin or thapsigargin results in one or more small spikes of Ca^{2+} in most, but not all cells, as shown in Fig. 5. These spontaneous spikes of Ca^{2+} entry have been observed previously in A7r5 cells and are mediated by L-type Ca^{2+} channels, since they are blocked by nimodipine or verapamil (39, 40). Since TRPC6 knockdown results in a significant loss of VP-induced Ca^{2+} entry, we may infer that the receptor-induced Ca^{2+} entry is partly, but not wholly, dependent on TRPC6 channels. As shown in Fig. 1, TRPC expression in A7r5 cells is certainly not restricted to TRPC6 alone; hence, the residual receptor-induced Ca^{2+} entry in cells after TRPC6 RNAi treatment may reflect the operation of other TRPC channels. An alternative interpretation is that the Ca^{2+} entry response induced by VP comprises discrete store-dependent and store-independent components. Whereas each of the seven mammalian TRPC channels have been implicated in mediating store-operated Ca^{2+} entry, in most cases, this is controversial with data both in favor and against such a role (reviewed in Refs. 1–3 and 13). The data shown in Fig. 5*A* provide good evidence against TRPC6 functioning in response to store emptying *per se*. Earlier, we reported that the closely related homologue, TRPC3, while activated by PLC-coupled receptors, was unaffected by stores (29, 30). In those studies, we utilized transient and stable overexpressing systems to examine TRPC3 function, and we speculated that, under such high expression conditions, TRPC3 channels may be "uncoupled" from stores while still activated by the PLC product, DAG (2, 11). The current results indicate that endogenously expressed TRPC6 channels also are not functioning as store-operated channels.

Effects of TRPC6 Knockdown on OAG-induced Ca^{2+} Entry—An obvious further experiment was to examine the actions of TRPC6 knockdown on any Ca^{2+} entry that was mediated by the direct TRPC6 activator, OAG. Indeed, the A7r5 cells showed a substantial increase in Ca^{2+} in response to OAG addition (Fig. 6*A*). This increased Ca^{2+} level was all due to entry, since there was no OAG-induced Ca^{2+} increase in the absence of extracellular Ca^{2+} (data not shown). Surprisingly, however, there was little change in this OAG-induced Ca^{2+} entry in A7r5 cells treated with siRNA for TRPC6 (Fig. 6*B*) as opposed to cells treated with control siRNA (Fig. 6*A*). We undertook a total of six individual experiments, each involving multiple separate traces (6–12 cells in each trace) of control RNA-treated cells or cells treated with either or both of the 1609 or 1574 TRPC6 siRNA sequences. From 11 TRPC6 siRNA traces, only one showed a significant decrease in OAG-induced Ca^{2+} entry from control-treated cells, one showed a slight decrease, and the remaining nine traces revealed no significant change. Based on the substantial TRPC6-mediated current activity (Fig. 4), this was an unexpected result.

Is OAG-induced Ca^{2+} Entry Mediated by TRPC6 Channels?—We sought to independently assess whether the OAG-induced Ca^{2+} entry was actually mediated by TRPC6. Since many actions of DAG are PKC-mediated, an obvious possibility was that OAG induced an effect through PKC. Therefore, we assessed any PKC role by utilizing the aminoalkyl bisindolylmaleimide, GF109203X, recognized as a potent inhibitor of multiple PKC subtypes (10, 41). Compared with control (Fig. 7*A*), there was no inhibition by GF109203X on OAG-induced Ca^{2+} entry; indeed, there was a slight enhancement at longer times (Fig. 7*B*). In fact, this slight longer term increase in OAG-induced entry was consistent with the action of PKC to inhibit TRPC channels (10). PKC-induced inhibition of the closely related TRPC3 channel (10) was a

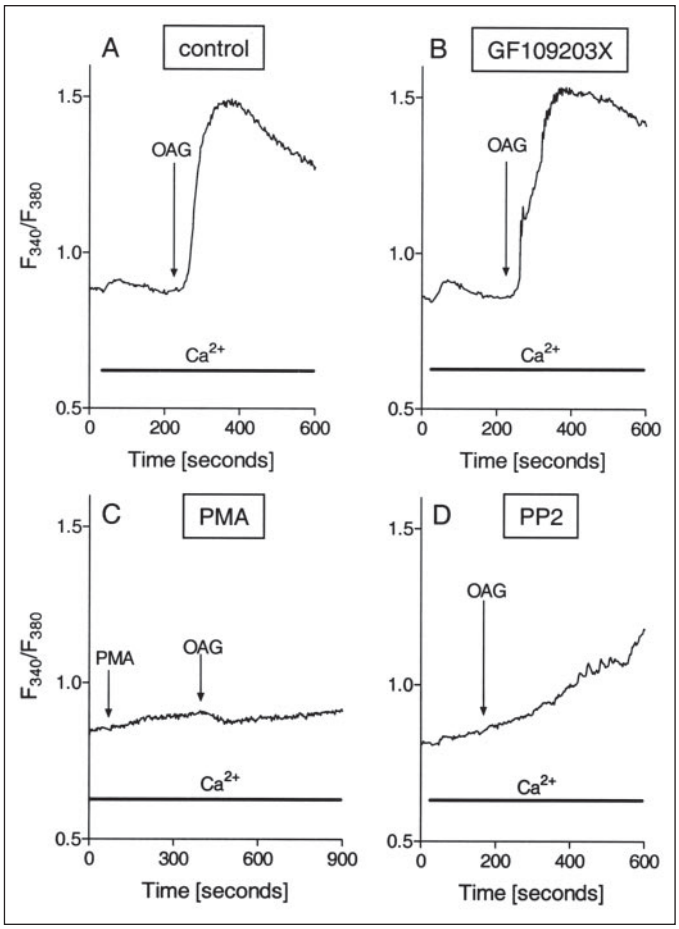

FIGURE 7. **OAG-induced Ca^{2+} entry has the pharmacological profile of TRPC6 channels.** A7r5 cells maintained under optimal growth conditions were loaded with fura-2. *A*, exposure to 100 μM OAG in the presence of 3 mM Ca^{2+} led to typical Ca^{2+} entry. *B*, the addition of the protein kinase C inhibitor GF-109203X at 10 μM did not block OAG-induced Ca^{2+} entry but caused a slight delay in the rate of Ca^{2+} entry deactivation. *C*, activation of PKC by 100 nM PMA completely blocked OAG-induced Ca^{2+} entry. *D*, preincubation (20 min) of cells with the Src-Yes-Fyn kinase family inhibitor PP2 (10 μM) substantially blocked OAG-induced Ca^{2+} entry. Inhibition by PKC activation and PP2 is consistent with the involvement of TRPC6 channels in OAG-induced Ca^{2+} entry.

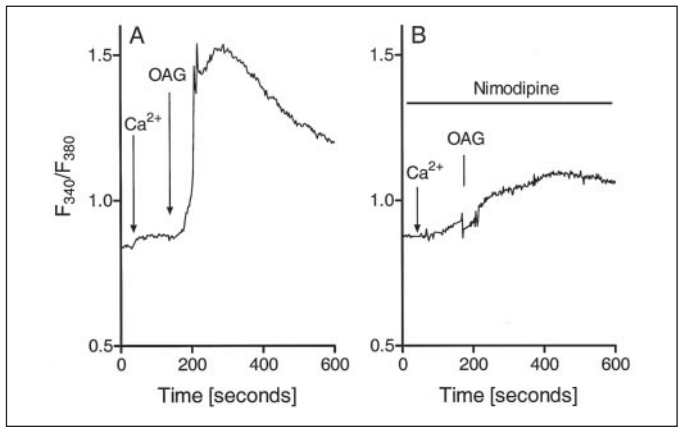

FIGURE 8. **OAG-induced Ca^{2+} entry in A7r5 cells is mediated by L-type Ca^{2+} channels.** A7r5 cells maintained under optimal growth conditions were loaded with Fura-2. *A*, exposure to 100 μM OAG in the presence of 3 mM Ca^{2+} led to typical Ca^{2+} entry. *B*, the potent and specific L-type Ca^{2+} channel inhibitor, nimodipine (1 μM), was added ~1 min prior to the addition of Ca^{2+}. Under these conditions, OAG-induced Ca^{2+} entry was strongly inhibited.

powerful effect and provided a functional "hallmark" in the identification of TRPC channels. We sought to assess the actions of prior treatment of A7r5 cells with the powerful PKC activator, PMA, which causes pronounced PKC-mediated phosphorylation of targets at nanomolar levels (10, 42). Using stably TRPC3-transfected HEK 293 cells, we previously determined that OAG-induced activation of TRPC3 was abolished by a 5-min pretreatment with PMA (10). As shown in Fig. 7*C*, using A7r5 cells, the same 5-min preincubation with 100 nM PMA resulted in a complete loss of the OAG-induced entry of Ca^{2+}. Our earlier studies also revealed that PKC activation completely blocked TRPC4 and TRPC5 channels, in addition to TRPC3 channels (10, 33). Given that TRPC6 channels are closely related to TRPC3 channels, that TRPC4 and TRPC5 channels are unaffected by OAG (9, 10), and that TRPC3 and TRPC7 channels are undetectable in A7r5, we draw a strong inference that OAG is inducing TRPC6 channel activation in A7r5 cells.

Whereas there are no specific modifiers of the TRPC6 channel that would provide definitive proof of its involvement, the recent finding that tyrosine phosphorylation by Src family protein-tyrosine kinases controls TRPC6 channel activity (43) provides a further useful identifying feature. Indeed, the specific inhibitor of Src family PTKs, PP2, was shown to abolish activation of TRPC6 channels (43) and the closely related TRPC3 channel (44). The results shown in Fig. 7*D* reveal that the OAG-induced Ca^{2+} entry is strongly inhibited by prior incubation with 10 μM PP2, consistent with its action on TRPC6 channels. Overall, based on observations in Fig. 7 that Ca^{2+} entry is activated by OAG independently of PKC, is blocked by PKC inhibition, and is inhibited by Src PTK inhibition, there is strong circumstantial evidence that OAG is inducing its action through TRPC6 channel activation.

Reconciliation: TRPC6 Channels Mediate L-type Channel Activation—The paradox emerging from the TRPC6 knockdown and TRPC6 functional studies appears to have a simple and physiologically important resolution. The experiment shown in Fig. 8 reveals that the OAG-induced entry of Ca^{2+} in A7r5 cells is largely blocked by the dihydropyridine L-type channel blocker, nimodipine. Compared with control OAG-induced Ca^{2+} entry (Fig. 8*A*), the addition of 1 μM nimodipine 1 min prior to the addition of Ca^{2+} resulted in a greatly attenuated Ca^{2+} entry response to OAG (Fig. 8*B*). Similar inhibition was observed with the nondihydropyridine L-type channel blocker, verapamil, at 10 μM (data not shown). This indicates that the entry of Ca^{2+} ions in response to OAG is mostly carried by L-type Ca^{2+} channels. This is in contrast to the electrophysiological measurements (Figs. 2 and 4), which were undertaken in the presence of nimodipine. TRPC channels, including TRPC6, are considered to be largely nonselective cation channels, the predominant inward current passing through them being attributed to Na^+ ions (4, 5, 45). A7r5 cells, like primary smooth muscle cells, are clearly established to express L-type Ca^{2+} channels, and their function has been well characterized in this cell line (39, 40, 46). The resting membrane potential of cultured A7r5 cells measured in several studies is in the −40 to −50-mV range (39, 46). The threshold for opening of L-type channels in A7r5 cells is in the −10 to −20-mV range, and peak Ca^{2+} current through L-type channels is observed at approximately +10 mV (39, 46). A relatively small current mediated by TRPC6 channels could result in effective L-type channel opening. It is clear that TRPC6 channels in A7r5 cells inactivate slowly ($\tau \sim 50$ s in Fig. 2), consistent with other studies (22). We approached the question of whether TRPC6 channels would be able to mediate membrane depolarization before they inactivate and how reducing the number of TRPC6 channels by 90% would change this. To estimate how fast the cell would be depolarized due to TRPC6 activation, we used the classical capacitance discharge equation,

$$V = V_r \exp\left(\frac{-t}{R_m C_m}\right) \qquad \text{(Eq. 1)}$$

in which V represents the membrane potential, V_r is the resting membrane potential, t is the time after maximum activation of TRPC6, and R_m is the membrane resistance (V_m/I_m) after maximal activation of TRPC6 channels. We used the value of −15 mV as the threshold (V_t) for L-type channels in A7r5 cells (39, 46). Based on our studies and those of others (5), the TRPC6 channel has minimal voltage gating and a reversal potential of 0 mV. To simplify calculations, we made the assumption that TRPC6 has a linear voltage dependence between −80 and 0 mV. We also assumed that no other channels become activated as a result of TRPC6 channel opening (either due to the Ca^{2+} influx or membrane depolarization to V_t) and hence that the membrane resistance R_m stays constant during the depolarization. Based on this, the time to reach V_t is given by the following equation.

$$t = -\frac{V_m}{I_m} C_m \ln \frac{V_t}{V_r} \qquad \text{(Eq. 2)}$$

Using the value for resting potential of −50 mV and our experimental data for I_m/C_m of −0.5 pA/picofarads at −80 mV, then t, the time to reach threshold potential, would be 192 ms. If we were to have reduced the total number of TRPC6 channels by 90%, then the time to reach threshold would be 1.92 s. This means that even with a substantial reduction in TRPC6 channels, the time to reach a potential at which L-type channels are opening would still be very rapid, and a change in L-type channel activation would escape detection in our Ca^{2+} imaging experiments.

One question arising from the data in Figs. 5 and 6 is the apparent discrepancy between the effects of RNAi for TRPC6 on the function of VP-induced as opposed to OAG-induced Ca^{2+} entry. Our experiments revealed that the entry of Ca^{2+} in response to VP was largely unaffected by L-type blockers (data not shown). This is explained by our own observations and those of others (39, 45, 47) that VP causes inhibition of L-type channels. In response to VP, the TRPC6 channel appears to be carrying a larger amount of Ca^{2+} (Fig. 5, *D* and *E*) than it does when activated by OAG in the presence of nimodipine (Fig. 8*B*). It is also clear that the *I*/V curve for VP-induced current (Fig. 2*B*) is distinct from the purely OAG-activated current (Fig. 4*B*), which more closely resembles the *I*/V curve for TRPC6 (5). One explanation for these differences is the existence of different populations of TRPC6 channels responding to OAG and vasopressin. In a previous study (48), heteromers between TRPC1, TRPC5 (or TRPC4), and TRPC6 were demonstrated in embryonic rat brain and in overexpression studies in HEK293 cells. These heteromers were activated by PLC-coupled receptors but *not* by OAG. Given the predominant expression of the same spectrum of TRPC proteins in A7r5 cells, the presence of such heteromers would be expected. Thus, whereas OAG may operate solely through TRPC6 homomers, the action of VP may also include the OAG-insensitive TRPC heteromers. This may explain the difference in the amount of Ca^{2+} entry carried by TRPC6 in response to VP as opposed to OAG. Our preliminary studies revealing TRPC6 immunoprecipitation with TRPC1 (data not shown) provide some support for this concept. Thus, whereas TRPC6 channels are a predominant species in A7r5 cells, interactions with other TRPC subtypes may result in multiple populations of channels with distinct activation properties.

Overall, we have combined targeted RNAi with a rigorous assessment of both message and protein, to provide new information on the presence and function of *endogenously* expressed TRPC6 channels in A7r5 cells. The results indicate that endogenous TRPC6 channels are not involved in store-operated Ca^{2+} entry but do contribute to the entry of Ca^{2+} following PLC-coupled receptor activation. Knockdown experiments reveal that an OAG-activated nonselective cation current is almost completely attributable to TRPC6. A corresponding TRPC6-mediated OAG-dependent entry of Ca^{2+} is not significantly altered by TRPC6 knockdown, and this entry is mostly through L-type channels. The TRPC6 channel is hence acting as a mediator between PLC-generated DAG and the activation of Ca^{2+} entry through L-type channels. A scheme depicting this signaling process is shown in Fig. 9. The effectiveness of TRPC6 is sufficient that, even after substantial reduction of channel protein by RNAi, it still allows L-type channel activation. The function of TRPC channels mediating depolarization and activation of L-type channels has also been indicated in other studies. Thus, in cerebral arteries, TRPC6 antisense treatment reduced pressure-induced depolarization and arterial constriction, suggesting that TRPC6 channels are activated as a result of pressure and may play an important role in the control of myogenic tone (49). Very recently, the TRPC3 channel, which is also expressed in cerebral arteries, was shown to mediate purinergic receptor-induced depolarization and contraction (50). Thus, members of the TRPC3/6/7 subfamily of nonselective cation channels may play an important role in the control of smooth muscle cell membrane potential to effect control over voltage-operated Ca^{2+} entry and muscle contraction.

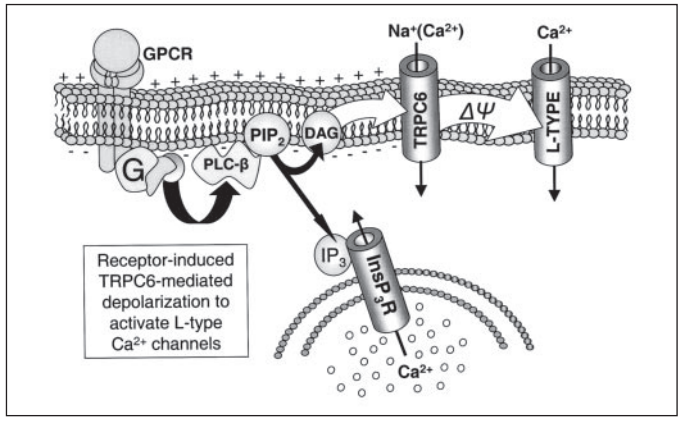

FIGURE 9. **Model to depict the role of TRPC6 channels in the coupling between receptor-induced PLC stimulation and L-type Ca^{2+} channel activation.** The G protein-coupled receptor (*GPCR*; *e.g.* the VP receptor) activates PLC-β via G protein (*G*) and results in the formation of DAG and $InsP_3$. Whereas $InsP_3$ induces Ca^{2+} release from stores, DAG activates the nonselective cation channel, TRPC6. The predominant entry of Na^+ ions (in addition to Ca^{2+} ions) results in depolarization of the membrane and the activation of voltage-sensitive L-type Ca^{2+} channels. $InsP_3R$, $InsP_3$ receptor.

Acknowledgments—We thank Dr. Stefanie Vogel for advice in real time PCR determinations and Thomas Crumbacker for expert technical assistance.

REFERENCES

1. Berridge, M. J., Bootman, M. D., and Roderick, H. L. (2003) *Nat. Rev. Mol. Cell. Biol.* **4,** 517–529
2. Venkatachalam, K., van Rossum, D. B., Patterson, R. L., Ma, H. T., and Gill, D. L. (2002) *Nat. Cell Biol.* **4,** E263–E272
3. Parekh, A. B., and Putney, J. W., Jr. (2005) *Physiol. Rev.* **85,** 757–810
4. Montell, C. (2005) *Sci. STKE 2005,* RE3
5. Clapham, D. E. (2003) *Nature* **426,** 517–524
6. Freichel, M., Vennekens, R., Olausson, J., Hoffmann, M., Muller, C., Stolz, S., Scheunemann, J., Weissgerber, P., and Flockerzi, V. (2004) *Biochem. Biophys. Res. Commun.* **322,** 1352–1358
7. Dietrich, A., Mederos, Y. S., Kalwa, H., Storch, U., and Gudermann, T. (2005) *Naunyn-Schmiedeberg's Arch. Pharmacol.* **371,** 257–265
8. Dietrich, A., Mederos, Y. S., Gollasch, M., Gross, V., Storch, U., Dubrovska, G., Obst, M., Yildirim, E., Salanova, B., Kalwa, H., Essin, K., Pinkenburg, O., Luft, F. C., Gudermann, T., and Birnbaumer, L. (2005) *Mol. Cell. Biol.* **25,** 6980–6989
9. Hofmann, T., Obukhov, A. G., Schaefer, M., Harteneck, C., Gudermann, T., and Schultz, G. (1999) *Nature* **397,** 259–263

10. Venkatachalam, K., Zheng, F., and Gill, D. L. (2003) *J. Biol. Chem.* **278,** 29031–29040
11. Spassova, M. A., Soboloff, J., He, L. P., Hewavitharana, T., Xu, W., Venkatachalam, K., van Rossum, D. B., Patterson, R. L., and Gill, D. L. (2004) *Biochim. Biophys. Acta* **1742,** 9–20
12. Lucas, P., Ukhanov, K., Leinders-Zufall, T., and Zufall, F. (2003) *Neuron* **40,** 551–561
13. Gudermann, T., Hofmann, T., Schnitzler, M., and Dietrich, A. (2004) *Novartis Found. Symp.* **258,** 103–118
14. Gill, D. L., and Patterson, R. L. (2004) *Sci. STKE 2004,* PE39
15. Gudermann, T., Schnitzler, M. M., and Dietrich, A. (2004) *Sci. STKE 2004,* PE35
16. Montell, C. (1999) *Annu. Rev. Cell Dev. Biol.* **15,** 231–268
17. Patterson, R. L., van Rossum, D. B., Ford, D. L., Hurt, K. J., Bae, S. S., Suh, P. G., Kurosaki, T., Snyder, S. H., and Gill, D. L. (2002) *Cell* **111,** 529–541
18. van Rossum, D. B., Patterson, R. L., Sharma, S., Barrow, R. K., Kornberg, M., Gill, D. L., and Snyder, S. H. (2005) *Nature* **434,** 99–104
19. Li, H.-S., Xu, X.-Z. S., and Montell, C. (1999) *Neuron* **24,** 261–273
20. Inoue, R., Okada, T., Onoue, H., Hara, Y., Shimizu, S., Naitoh, S., Ito, Y., and Mori, Y. (2001) *Circ. Res.* **88,** 325–332
21. Yu, Y., Sweeney, M., Zhang, S., Platoshyn, O., Landsberg, J., Rothman, A., and Yuan, J. X. (2003) *Am. J. Physiol.* **284,** C316–C330
22. Jung, S., Strotmann, R., Schultz, G., and Plant, T. D. (2002) *Am. J. Physiol.* **282,** C347–C359
23. Albert, A. P., and Large, W. A. (2003) *J. Physiol.* **552,** 789–795
24. Mederos y Schnitzler, Y., Storch, U., Dietrich, A., and Gudermann, T. (2005) *Naunyn-Schmiedeberg's Arch. Pharmacol.* **369,** Suppl. 1, R62 (abstr.)
25. He, L. P., Hewavitharana, T., Soboloff, J., Spassova, M. A., and Gill, D. L. (2005) *J. Biol. Chem.* **280,** 10997–11006
26. Livak, K. J., and Schmittgen, T. D. (2001) *Methods* **25,** 402–408
27. Laemmli, U. K. (1970) *Nature* **227,** 680–685
28. Towbin, H., and Gordon, J. (1984) *J. Immunol. Methods* **72,** 313–340
29. Ma, H.-T., Patterson, R. L., van Rossum, D. B., Birnbaumer, L., Mikoshiba, K., and Gill, D. L. (2000) *Science* **287,** 1647–1651
30. Venkatachalam, K., Ma, H. T., Ford, D. L., and Gill, D. L. (2001) *J. Biol. Chem.* **276,** 33980–33985
31. Ma, H. T., Venkatachalam, K., Parys, J. B., and Gill, D. L. (2002) *J. Biol. Chem.* **277,** 6915–6922
32. Patterson, R. L., van Rossum, D. B., and Gill, D. L. (1999) *Cell* **98,** 487–499
33. Venkatachalam, K., Zheng, F., and Gill, D. L. (2004) *Novartis Found. Symp.* **258,** 172–185
34. Chu, X., Cheung, J. Y., Barber, D. L., Birnbaumer, L., Rothblum, L. I., Conrad, K., Abrasonis, V., Chan, Y. M., Stahl, R., Carey, D. J., and Miller, B. A. (2002) *J. Biol. Chem.* **277,** 34375–34382
35. Jungnickel, M. K., Marrero, H., Birnbaumer, L., Lemos, J. R., and Florman, H. M. (2001) *Nat. Cell Biol.* **3,** 499–502
36. Moneer, Z., Pino, I., Taylor, E. J., Broad, L. M., Liu, Y., Tovey, S. C., Staali, L., and Taylor, C. W. (2005) *Biochem. J.* **389,** 821–829
37. Seth, M., Sumbilla, C., Mullen, S. P., Lewis, D., Klein, M. G., Hussain, A., Soboloff, J., Gill, D. L., and Inesi, G. (2004) *Proc. Natl. Acad. Sci. U. S. A.* **101,** 16683–16688
38. van Rossum, D. B., Patterson, R. L., Kiselyov, K., Boehning, D., Barrow, R. K., Gill, D. L., and Snyder, S. H. (2004) *Proc. Natl. Acad. Sci. U. S. A.* **101,** 2323–2327
39. Van Renterghem, C., Romey, G., and Lazdunski, M. (1988) *Proc. Natl. Acad. Sci. U. S. A.* **85,** 9365–9369
40. Byron, K. L., and Taylor, C. W. (1993) *J. Biol. Chem.* **268,** 6945–6952
41. Toullec, D., Pianetti, P., Coste, H., Bellevergue, P., Grand-Perret, T., Ajakane, M., Baudet, V., Boissin, P., Boursier, E., and Loriolle, F. (1991) *J. Biol. Chem.* **266,** 15771–15781
42. Quest, A. F., Ghosh, S., Xie, W. Q., and Bell, R. M. (1997) *Adv. Exp. Med. Biol.* **400A,** 297–303
43. Hisatsune, C., Kuroda, Y., Nakamura, K., Inoue, T., Nakamura, T., Michikawa, T., Mizutani, A., and Mikoshiba, K. (2004) *J. Biol. Chem.* **279,** 18887–18894
44. Vazquez, G., Wedel, B. J., Kawasaki, B. T., Bird, G. S., and Putney, J. W., Jr. (2004) *J. Biol. Chem.* **279,** 40521–40528
45. Schuhmann, K., Romanin, C., Baumgartner, W., and Groschner, K. (1997) *J. Gen. Physiol* **110,** 503–513
46. Gollasch, M., Haase, H., Ried, C., Lindschau, C., Morano, I., Luft, F. C., and Haller, H. (1998) *FASEB J.* **12,** 593–601
47. Poteser, M., Wakabayashi, I., Rosker, C., Teubl, M., Schindl, R., Soldatov, N. M., Romanin, C., and Groschner, K. (2003) *Circ. Res.* **92,** 888–896
48. Strubing, C., Krapivinsky, G., Krapivinsky, L., and Clapham, D. E. (2003) *J. Biol. Chem.* **278,** 39014–39019
49. Welsh, D. G., Morielli, A. D., Nelson, M. T., and Brayden, J. E. (2002) *Circ. Res.* **90,** 248–250
50. Reading, S. A., Earley, S., Waldron, B. J., Welsh, D. G., and Brayden, J. E. (2005) *Am. J. Physiol.* **288,** H2055–H2061